Optimal Heating Strategies of Polymer Binder Burnout Process Using Dynamic Optimization Scheme

Leo Chau-Kuang Liau* and Chi-Chong Chiu

Department of Chemical Engineering and Materials Science, Yuan Ze University, Chung-Li 320, Taiwan

The dynamic optimization of polymer binder burnout processes was evaluated for a 3D cubic ceramic body in different sample porosities and atmospheres. Optimal heating trajectories of the binder removal processes to minimize the burnout time were estimated by the proposed algorithm. The process model can be constructed by the chemical kinetics of the polymer burnout and the mass transport of the volatile gas evolved from polymer burnout inside the ceramic body. A numerical simulation was used to calculate the buildup pressure distribution formed by the volatile gas which affects the generation of the ceramic defects. The results show that the maximum pressure was found at the body center through the binder burnout period. The process needs to be well-controlled to avoid the formation of a large buildup pressure, especially for the samples with small porosities, during the initial binder burnout stages. In addition, the effects of the operating atmospheres and the sample porosities on the optimal heating trajectories were discussed.

Introduction

Ceramic components are usually produced from laminated green ceramics treated through a thermal cycle. In general, the green ceramic components consist of ceramic powders mixed with solvents, organic dispersants, and polymer binders to enhance their mechanical strength for forming capability. The organic materials have to be removed in the initial stages of the thermal cycle. The removal of the polymer binders, or so-called binder burnout, takes a long time and plays an important role in the defect formation of the ceramic body during the ceramic manufacturing process. Therefore, the binder burnout process has to be operated and controlled in an optimal heating strategy to obtain better quality and a higher yield of the products.

The ceramic components generate defects, such as cracking, blistering, and warping, during the thermal treatments. One of the critical factors to form the defects is attributed to the inappropriate setting of a heating strategy in the binder removal process. Lewis[1] reported that the removal process involves complex chemical and physical phenomena inside the ceramic body. The main theories of these phenomena were focused on the kinetics of polymer binder degradation and the mass transport of the degraded gas diffusing out of the ceramic body. Therefore, the fundamental knowledge of the binder removal phenomena corresponding to the heating conditions has to be well-understood to avoid the defect formation.

The kinetics of polymer/ceramic thermal degradation was studied associated with several parameters, such as polymer binder composition, degradation gas chemistry, and different ceramic surface interactions.[1] The effects of these parameters on the polymer thermal degradation were analyzed using several analytical techniques, such as thermogravimetry (TG), Fourier transform infrared spectroscopy (FT−IR), mass spectrometry (MS), and gel permeation chromatography (GPC).[2−4] The composition effects of ceramic and metal on poly(vinyl butyral) (PVB) binder thermal degradation were discussed by Liau et al.[5] The volatile products of the polymer degradation were resolved, and the kinetics of the degradation reaction was analyzed by data measured from these analytical techniques.[2,6] The polymer degradation mechanisms and kinetic parameters of the Arrhenius equation were determined in their studies. The surface interactions, such as the catalytic effects of different ceramics on polymer binder degradation, were discussed from the studies.[5,7]

The investigations of the physical phenomena of the polymer binder removal were focused on the mass transport of the volatile gas during the polymer burnout period. The mechanistic description of the volatile gas diffusing from inside the void space of the ceramic to the body surface was reported.[1] The volatile gas fluid flow was taken as a critical component of the generation of the internal pressure buildup and the stresses affecting a ceramic body.[8] These forces have a critical influence on the formation of the defects and failures on the body. The fluid flow model of the gaseous products inside a porous media had been mathematically developed in three-dimensional space and assumed uniform temperature distribution inside a cubic ceramic body.[9] The distribution of the internal pressure and stresses within the cubic body were numerically solved using the flow model and the kinetics of the binder burnout in their studies.[9,10] Moreover, the distribution of these internal forces was affected by several conditions, such as the heating conditions and the kinetics of polymer binder degradation.

In recent years, dynamic optimization and optimal control techniques were extensively applied on industrial engineering processes to improve the profit and product quality effectively. Many industrial processes, such as polymerization,[11] electrochemical reaction,[12] and crystallization,[13] were studied to determine the operating trajectories of their dynamic optimization. To carry out the optimization scheme, the process model or system data used to describe the process have to be

* Corresponding author. Tel.: 886-3-463-8800 ext. 573. Fax: 886−3−455-9373. E-mail: lckliau@saturn.yzu.edu.tw.

10.1021/ie049143a CCC: $30.25
Published on Web 05/20/2005

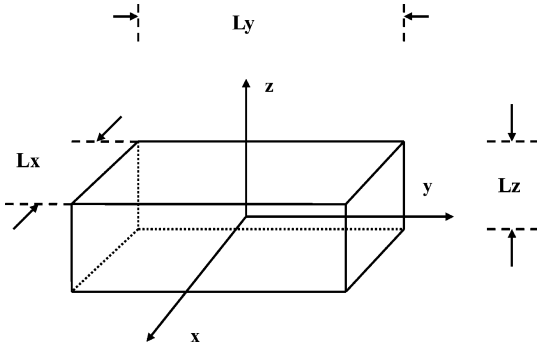

Figure 1. Geometry of the ceramic cubic and the coordinate system.

obtained and built. The process model together with optimization approaches was applied to solve a dynamic optimization problem. Maximum profits corresponding to a defined objective function, i.e., minimum operating time, were evaluated using a dynamic optimization scheme. In the ceramic manufacturing process, the fabrication of ceramic components needs several days to complete the thermal cycles to maintain the required product quality. If the binder removal process can be optimized dynamically, the quality of the ceramic product can be promoted and the operating cost and time can be reduced. However, little research has been done on the dynamic optimization and optimal control of the binder removal process.

In this study, the optimal trajectories of the heating rate or temperature for the polymer burnout process were evaluated with constraints using the proposed optimization scheme. The 3D process model of evolved gas transports and kinetics of polymer degradation combined with an optimization method was applied to search for the optimal heating trajectories. The effects of the sample porosities and operating environments on the optimal heating trajectories were discussed.

Dynamic Optimization Method

The dynamic optimization problem can be solved using an optimization scheme with a 3D model of the binder burnout process. The process model can be described by the chemical and physical theories of the polymer removal phenomena. The kinetics of polymer degradation is a way to express the chemical description, and the mass transport of the evolved gas generated from the polymer degradation is involved in the system.

The temperature inside the polymer/ceramic sample can distribute nonisothermally from a heat transport perspective. The polymer degradation reaction can be affected by the temperature distribution. However, if the temperature difference inside the small sample body (1 cm × 2 cm × 1 cm) is not significant due to the slow temperature ramping during the burnout period, then the temperature distribution is approximately uniform. Therefore, the model may be simplified and treated isothermally in this work. The optimal control algorithm can be developed as follows.

1. Equation of Continuity. The flow system in 3D directions for the evolved gas in a cubic ceramic body as depicted in Figure 1 is described as

$$\frac{\partial(\rho v_g)}{\partial t} = -\left[\frac{\partial}{\partial x}(\rho u_x) + \frac{\partial}{\partial y}(\rho u_y) + \frac{\partial}{\partial z}(\rho u_z)\right] + \frac{r}{M} \quad (1)$$

where ρ is the molar density, M is the average molecular weight, u_i is the flow rate in the i direction, and r is the decomposition rate. The flow rate in porous media can be expressed using Darcy's Law

$$u_i = -\frac{\kappa_i}{\mu}\frac{\partial P}{\partial i} \quad (2)$$

where μ is the fluid viscosity, P is the pressure, and κ_i is the diffusion coefficient described using the Kozeny–Carman equation as

$$\kappa_i = \frac{{v_g}^3}{k_i(1 - v_g)^2 S^2} \quad (3)$$

where k_i is a constant related to the shape and tortuosity of the pores and S is the surface area per unit volume of the ceramic body. It is assumed that the S and k_i (typically between 3 and 7) values remain constant due to the small pore size and high ceramic composition of the sample to simplify the determination of the parameters. From Darcy's law, the fluid flow can be assumed as a laminar and slip flow if the ratio of the mean free path to the porosity radius is <1.

If ideal gas law is assumed, then the molar density can be expressed as

$$P = \rho RT \quad (4)$$

If it is assumed that the viscosity of the fluid was fixed, the definition of the dimensionless groups is

$$\bar{x} = \frac{2x}{L_x}$$

$$\bar{y} = \sqrt{\frac{\kappa_x}{\kappa_y}}\frac{2y}{L_x}$$

$$\bar{z} = \sqrt{\frac{\kappa_x}{\kappa_z}}\frac{2z}{L_x}$$

$$\bar{\rho} = \frac{\rho}{\rho_0}$$

$$\bar{t} = \frac{t}{\gamma} \quad (5)$$

where ρ_0 is the initial density of the decomposed gas and γ is the fluid flow time constant defined as

$$\gamma = \frac{\mu\kappa_x S^2 {L_x}^2}{P_0} \quad (6)$$

Eq 1 can be transformed into the dimensionless equation

$$\left(\frac{C}{2}\right)\left(\frac{\rho_0 M}{\rho_b}\right)\bar{\rho} + \left(\frac{(1 - v_g)^2}{4{v_g}^2}\right)\left(\frac{T_0}{T}\right)\left(\frac{\partial\bar{\rho}}{\partial\bar{t}}\right) = \bar{\rho}\left(\frac{\partial^2\bar{\rho}}{\partial\bar{x}^2}\right) + \left(\frac{\partial\bar{\rho}}{\partial\bar{x}}\right)^2 + \bar{\rho}\left(\frac{\partial^2\bar{\rho}}{\partial\bar{y}^2}\right) + \left(\frac{\partial\bar{\rho}}{\partial\bar{y}}\right)^2 + \bar{\rho}\left(\frac{\partial^2\bar{\rho}}{\partial\bar{z}^2}\right) + \left(\frac{\partial\bar{\rho}}{\partial\bar{z}}\right)^2 + \frac{C}{2} \quad (7)$$

where C is defined as

$$C = \left(\frac{L_x^2}{2\rho_0^2 \kappa_x}\right)\left(\frac{\mu}{RT}\right)\left(\frac{r}{M}\right) \tag{8}$$

The initial and boundary conditions are

$$\text{I.C.} \quad \bar{t} = 0 \qquad \bar{\rho} = 1$$

$$\text{B.C.} \quad \bar{x} = 0 \qquad \frac{\partial \bar{\rho}}{\partial x} = 0$$

$$\bar{x} = 1 \qquad \bar{\rho} = \frac{T_0}{T}$$

$$y = 0 \qquad \frac{\partial \bar{\rho}}{\partial x} = 0$$

$$\bar{y} = \frac{L_y}{L_x} \qquad \bar{\rho} = \frac{T_0}{T}$$

$$\bar{z} = 0 \qquad \frac{\partial \bar{\rho}}{\partial x} = 0$$

$$\bar{z} = \frac{L_z}{L_x} \qquad \bar{\rho} = \frac{T_0}{T} \tag{9}$$

For detailed explanations of the equation derivation, refer to ref 9.

2. Kinetic Equation of Polymer Degradation. The decomposition rate can be expressed as

$$r = \frac{\mathrm{d}\alpha}{\mathrm{d}t} = k_0 \exp\left(-\frac{E_a}{RT}\right)(1-\alpha)^n \tag{10}$$

where α is the binder conversion. If we let $\beta = \mathrm{d}T/\mathrm{d}t$, then eq 10 becomes

$$r = \frac{\mathrm{d}\alpha}{\mathrm{d}T} = k_0 \exp\left(-\frac{E_a}{RT}\right)(1-\alpha)^n/\beta \tag{11}$$

We can also replace α using ρ_b and the volumetric ratio of the binder v_b

$$r = -\frac{\mathrm{d}(\rho_b v_b)}{\mathrm{d}T} = k_0 \exp\left(-\frac{E_a}{RT}\right)\left(\frac{v_b}{v_{b0}}\right)^n \rho_b v_{b0}/\beta \tag{12}$$

and

$$v_b = v_{b0} - \int_0^t \frac{r}{\rho_b}\,\mathrm{d}t \tag{13}$$

where v_{b0} is the initial volumetric ratio of the binder. The binder density, ρ_b, is taken as a constant in this work. The volumetric relationship among the volatile gas, the ceramic, and the binder is

$$v_g = 1 - v_s - v_b \tag{14}$$

where v_s is the volumetric ratio of the ceramic.

3. Dynamic Optimization Scheme. The optimal control problem in this work is described as

$$\min_{\beta} t_f$$

$$\text{such that} \quad \beta = \frac{\mathrm{d}T}{\mathrm{d}t}$$

$$g(T,x) = 0$$

$$h(T,x) \le 0 \tag{15}$$

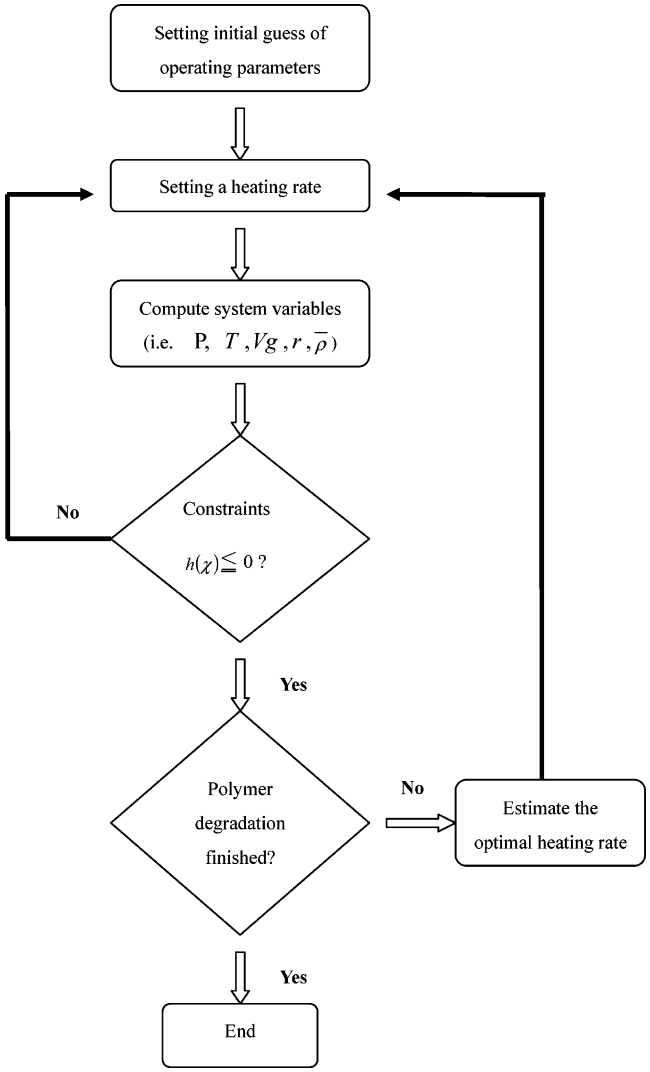

Figure 2. Schematic plot of the flow diagram for solving the dynamic optimization problem.

where T is the temperature, x is the operating variable, g is the process model, and h is the inequality constraint. The process model can be expressed by the use of the continuity equation and the kinetic equation of the polymer decomposition as described above. This problem can be numerically solved using the finite-difference method with the Crank−Nicholson algorithm to simulate the pressure distribution inside a 3D ceramic body. A cubic size of 1 cm × 2 cm × 1 cm is selected for the simulation study corresponding to 10 grid points for each dimension in the finite-difference calculation. The optimization approach utilized the successive quadratic programming (SQP) method for which programming was provided by MATLAB Corp. The flowchart for solving the dynamic optimization problem was proposed and is shown in Figure 2.

Results and Discussion

The distribution of the internal pressure buildup inside the ceramic body was numerically solved using the 3D process model. The generation of pressure buildup, which needs to be controlled to avoid the ceramic defect formation, is the constraint for the dynamic optimization problem. The optimal heating trajectories according to the operating conditions were evaluated using the proposed dynamic optimization scheme.

Table 1. Operating Parameters for the Process Simulation

	T_0		300 K
	P_0		0.1 MPa
	v_s		0.405
	v_{b0}		0.405
	v_{g0}		0.19
	β		0.5, 1, 2.5, 10 K/min
	ρ_b		1100 kg/m^3
	μ		0.025×10^{-3} Pa·s
	S		6×10^6 m^{-1}
	k_i		5
	L_x, L_y, L_z		2, 4, 1[a] cm or 1, 2, 1[b] cm
M	0.044[a] kg/mol	N_2	0.072[b] kg/mol
		air	$\alpha \le 0.5$, 0.072[b] kg/mol
			$\alpha > 0.5$, 0.046[b] kg/mol

[a] For case 1. [b] For case 2.

Table 2. Kinetic Parameters of the Thermal Decomposition of PVB/Ceramic Samples Determined Using TG Data in Different Environments. For case 1. E_a = 151.05 kJ/mol, n =1, ln(A) = 36.68 s^{-1}. For case 2.

	α	0−0.2	0.3	0.4	0.5	0.6	0.7	0.8−1
N_2	E_a (kJ/mol)	176.8	183.5	183.3	182.3	188.0	187.1	264.1
	n	−1.79	−2.65	0.70	1.60	1.58	2.97	5.12
	ln(A) (s^{-1})	30.0	30.9	31.3	31.5	32.4	33.4	50.3
air	E_a (kJ/mol)	137.9	133.0	130.4	110.8	140.9	210.5	203.5
	n	−0.084	9.72	7.25	10.01	14.94	8.80	4.73
	ln(A) (s^{-1})	28.3	29.3	28.2	25.3	36.0	42.4	35.5

1. Process Simulation of Binder Burnout Process. Case 1: Polymer Binder Burnout. The burnout of a ceramic cubic as illustrated in Figure 1 is used to demonstrate the calculation result compared with the work of Feng and Lombardo.[9] The operating parameters of this case are listed in Tables 1 and 2. Figure 3 shows the pressure distribution in the 3D cubic at 430 K with a heating rate of 10 K/min. The maximum pressure buildup formed inside the ceramic body was observed at the center during the polymer binder degradation. The pressure drop, which generates the internal stress on the ceramic body, is also an important factor to be considered in the burnout process. The highest pressure drop region is found near the body edge for the burnout process in Figure 3. Figure 4 demonstrates the pressure distribution if a lower heating rate of 1 K/min is applied for the burnout process. The maximum values of both pressure buildup at the center and the pressure drop near the cubic edge observed in Figure 4 can dramatically decrease. Figure 5 shows the pressure distributions at the cubic center, associated with the temperature at different heating rates. This indicates that higher heating rates can produce a large gas pressure at higher temperatures at the cubic center, where the binder degradation rate can be accelerated. In addition, the pressure drop between the center and the edge appears significant for higher heating rates due to the generation of the faster reaction rate. This result is in agreement with the previous investigation.[9]

2. Case 2: PVB/Ceramic Burnout. A sample of 30 wt % poly(vinyl butyral) (PVB) and 70% glass ceramic ($P_{30}C_{70}$) composite body was used for the study. The kinetics of this case, analyzed in nitrogen and air environments, were investigated in our previous studies.[14] The kinetic data used in this case are listed in Table 2 according to the kinetic analysis. The differences between the two operating environments are due to their degradation mechanisms. The degradation rates are higher at low temperatures for the burnout case in air than for that in nitrogen, especially for the large heating rate cases. This indicates that a larger amount of evolved gas is generated at lower temperature for the air case than for the nitrogen case. Figure 6 depicts the pressure distribution for different heating rates in nitrogen and air. The significant difference is that the maximum pressure was generated at a lower temperature in air than in nitrogen due to the effect of the degradation kinetic.

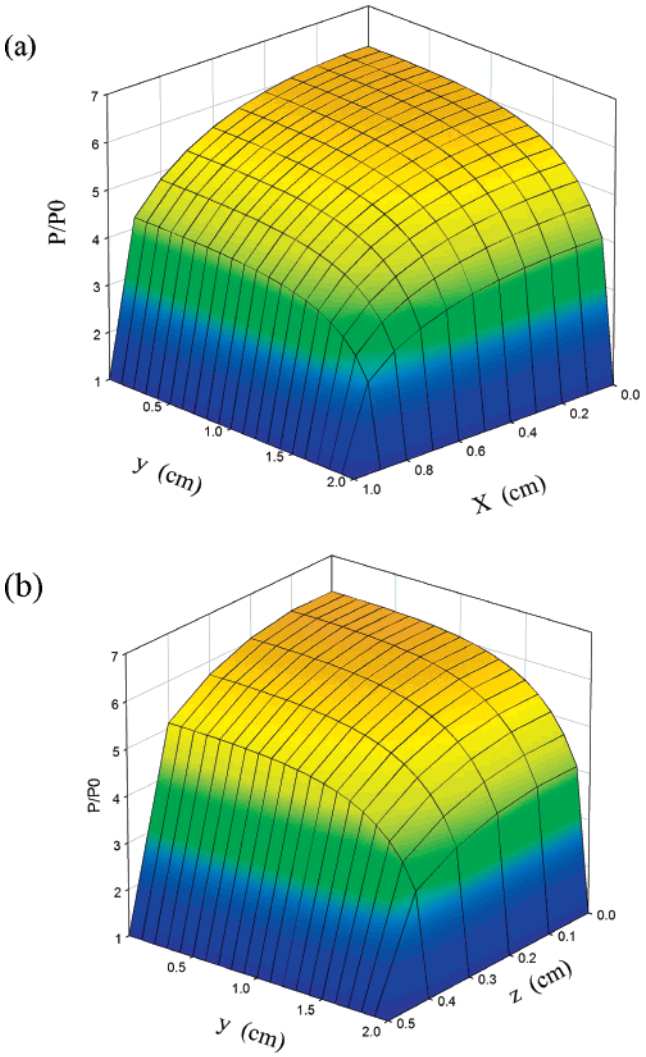

Figure 3. Distribution of the pressure in the cubic at 403 K with the heating rate at 10 K/min for case 1.

The initial porosity (v_{g0}) of the green ceramic is one of the critical parameters to affect the pressure buildup values during the polymer binder removal. Figure 7 shows the pressure distribution at 10 K/min when v_{g0} is varied from 0.19 to 0.1. The pressure for the case of v_{g0} = 0.1 increased more rapidly and earlier to its maximum point than that of the case of v_{g0} = 0.19. The maximum pressure appears more than double when v_{g0} becomes smaller, as illuminated in Figure 7. This is because the pores of the green ceramic cubic body are the only empty space to transport the gas in the beginning of the burnout period. Therefore, a small amount of the evolved gas can generate a large pressure buildup at this moment. This implies that the heating rate has to be controlled slowly and carefully enough to avoid the presence of a large pressure buildup during the early burnout period. This also indicates that the

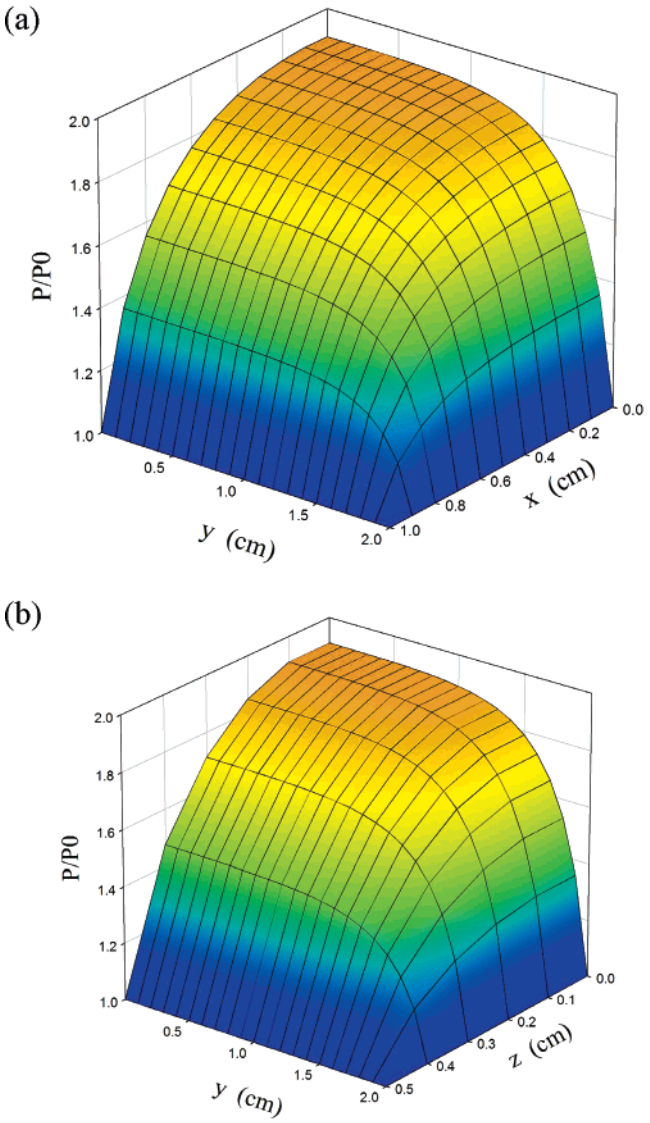

Figure 4. Distribution of the pressure in the cubic at 410 K with the heating rate at 1 K/min for case 1.

pressure buildup is sensitive to the variation of the sample property.

3. Dynamic Optimization of the Burnout Process. The dynamic optimization problem of polymer binder removal is stated as to minimize the required time to remove the polymer binder inside the ceramic cubic body by controlling the heating rate under constraints. The inequality constraints are set to limit the maximum pressure formation and the pressure difference with respect to time (dP/dt) inside the cubic body. The optimization problem can be expressed as

$$\min_{\beta} t_f$$

$$\text{such that} \qquad \beta = \frac{dT}{dt}$$

$$g(T,x) = 0$$

$$\frac{P}{P_0} \le 3.0$$

$$\frac{dP}{dt} \le 0.035 \qquad (16)$$

where t_f is the total time required to remove the polymer binder and g represents the model as shown in eqs 9, 12, and 13.

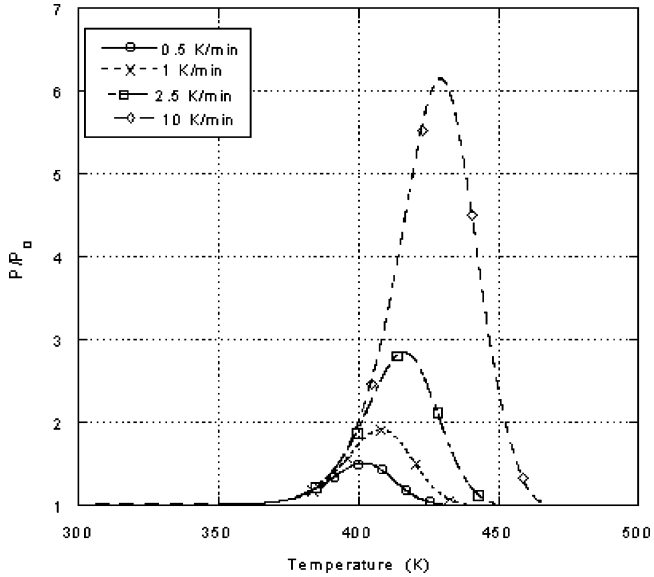

Figure 5. Distribution of the pressure at the cubic center with different heating rates for case 1.

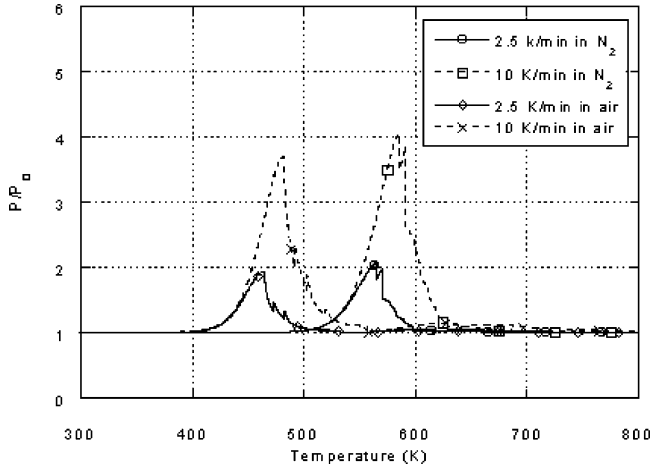

Figure 6. Distribution of the pressure at the cubic center with different heating rates and atmospheres for the $P_{30}C_{70}$ sample.

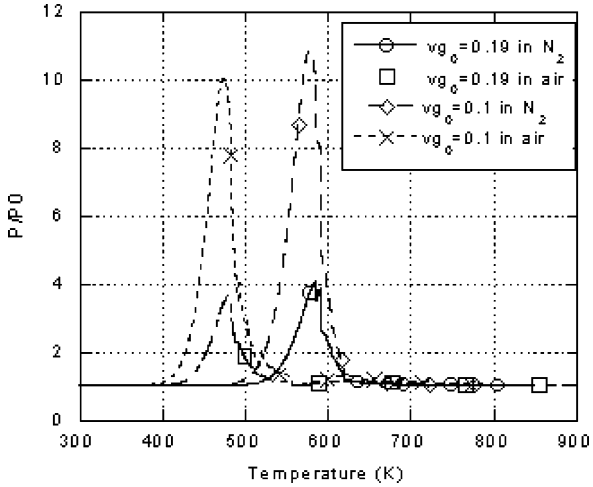

Figure 7. Distribution of the pressure at the cubic center with different porosities (v_{g0}) and atmospheres for the $P_{30}C_{70}$ sample.

Figure 8 shows the optimal trajectories of the heating rates for the thermal degradation of the $P_{30}C_{70}$ samples

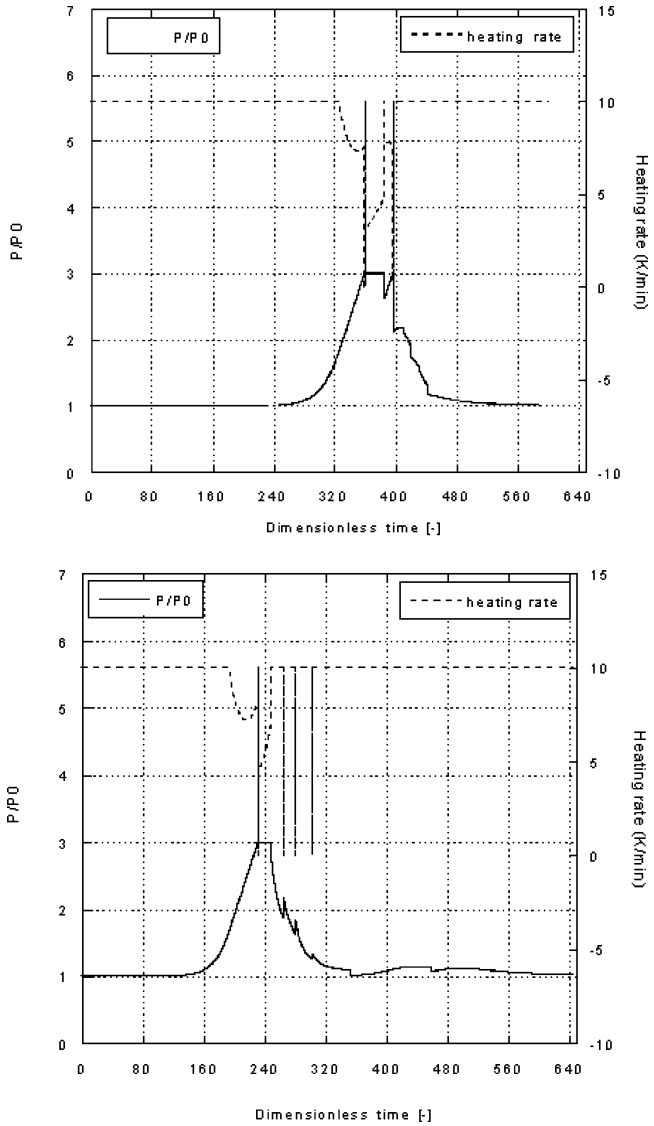

Figure 8. Optimal trajectories of optimal heating rate and distribution of the pressure at the cubic center for the $P_{30}C_{70}$ samples with $v_{g0} = 0.19$ operating in (a) nitrogen and (b) air.

with $v_{g0} = 0.19$ in nitrogen and air environments. The trajectories elucidate distinct pathways due to the effect of different operating environments on the mechanisms of PVB thermal degradation. The initial heating rate setting is at the maximum value (10 K/min) to proceed until the pressure rises in the main burnout period. The heating rate decreases at the time between 320 and 400 in nitrogen and between 180 and 320 in air as shown in parts a and b of Figure 8, respectively. In this period, the heating rate was optimally adjusted to satisfy the constraints of the optimization problem. After this major burnout period, the heating rate goes up to the maximum setting value. It is estimated that the time required to remove the polymer binder is longer for the process operating in air than for that in nitrogen as illustrated in Figure 8.

The dynamic optimization problem with the same constraints was solved for the sample of $v_{g0} = 0.1$. Figure 9 shows the optimal trajectories of the heating rate for the sample burnout in nitrogen and air atmospheres. In Figure 9a, the heating rate decreases rapidly from 10 K/min down to 0 K/min when the time is at ~300 to satisfy the constraint of pressure limitation in

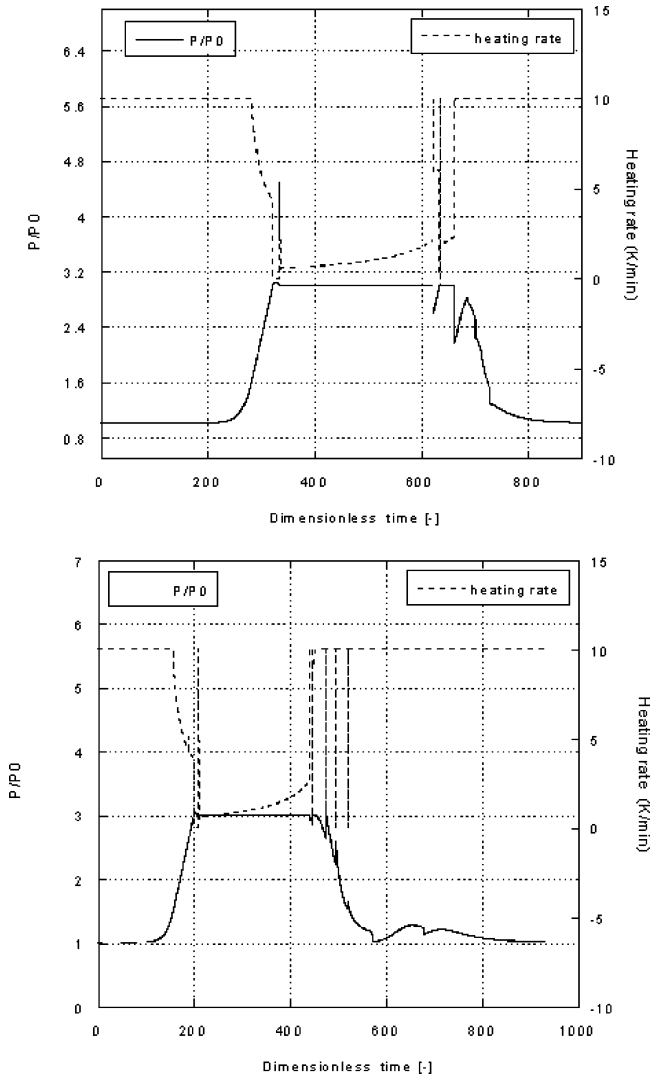

Figure 9. Optimal trajectories of optimal heating rate and distribution of the pressure at the cubic center for the $P_{30}C_{70}$ samples with $v_{g0} = 0.1$ operating in (a) nitrogen and (b) air.

nitrogen. The heating rate rises slowly to keep the pressure under the limitation for the time from 300 to 600. After the time reaches 650, the heating rate is accelerated to the maximum value and maintained to the end of the process, while in air, the optimal trajectory of the heating rate is similar to the case in nitrogen. However, the significant difference is that the time when the heating rate goes down to zero is shifted about 130 units earlier than that in nitrogen, as shown in Figure 9b. In addition, the burnout time when operating in air takes about 50 units longer than that in nitrogen.

The porosity of the green samples (v_{g0}) demonstrates a significant factor for affecting the optimal heating trajectory to remove the binder under the constraints. Figure 10 shows the temperature distribution of the optimal heating trajectories for the sample porosities and operating atmospheres. The optimal trajectories of the heating temperature were greatly influenced by the sample porosity. Longer optimal burnout times are needed for a smaller sample porosity ($v_{g0} = 0.1$) in both nitrogen and air to satisfy the operating constraints. For these samples, the operating temperature is maintained at ~450 K for 200 time units in air and goes up to 820 K in the end, while in nitrogen, the temperature is kept

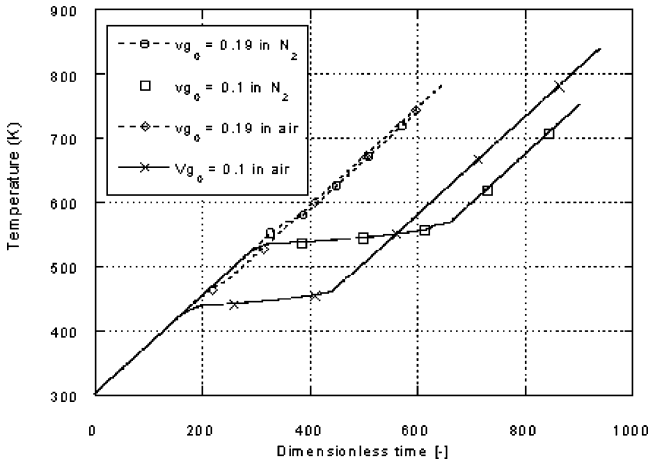

Figure 10. Optimal temperature trajectories determined in different conditions for the $P_{30}C_{70}$ samples.

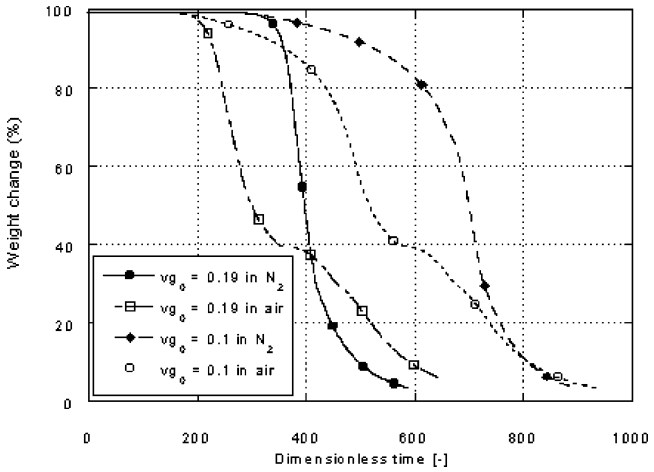

Figure 11. Optimal weight changes of the $P_{30}C_{70}$ samples thermally degraded in different conditions.

at 550 K for 350 time units and finally increases to ~750 K. Although the burnout reaction in air is faster at lower temperatures than the one in nitrogen, higher temperatures, beyond 800 K, are required to oxidize the carbonaceous residues during the last degradation stage.[5] In addition, the burnout effect of these operating atmospheres is due to the distinct mechanisms of PVB thermal degradation.

The optimal binder weight change of the $P_{30}C_{70}$ samples corresponding to the optimal heating strategies is illustrated in Figure 11 for different operating conditions. The distribution of the weight change was optimally controlled by the determined heating trajectories, as shown in Figure 10. The apparent difference due to the porosity effect is the different weight change paths in the initial weight change region, as elucidated in Figure 11. The rate of the weight change (slope) indicates the generation rate of the volatile gas during the binder burnout. For the smaller sample porosity, a large buildup pressure was significantly formed, even for a very small amount of the gas generated in the initial burnout stage. This is because the pores of the green body are the only empty space to transport the gas. This implies that slow burnout rates have to be controlled to avoid a large formation of buildup pressure in this stage. After some polymer binder was removed for a period of time, the volatile gas can take up both porous and devoid binder regions inside the ceramic body. The formation of the buildup pressure can be reduced when the effective empty volume is present. Therefore, the operation in the initial binder burnout stage needs to be controlled optimally and carefully to avoid large buildup pressure generation.

Conclusions

The optimal heating trajectories of the polymer binder burnout process were determined by numerical computation using the proposed dynamic optimization scheme. The minimum time needed to remove the polymer binder was evaluated under the constraint of the buildup pressure generation by the optimal heating strategy. The optimal heating strategy depends on the kinetics of binder removal and mass transport of the volatile gas during the burnout process. The buildup pressure distribution affected by the heating conditions can be optimally controlled using the determined optimal heating trajectory. Results show that the optimal strategy was greatly affected by the green ceramic sample porosities and the burnout atmospheres. The maximum buildup pressure was observed at the cubic center through the binder burnout process. The initial stage of binder removal needs to be carefully controlled to avoid large buildup pressure formation, especially for the samples with smaller porosity. In addition, the binder burnout takes a longer time and needs to be treated at a higher temperature to oxidize the carbonaceous residues in air than in nitrogen.

Acknowledgment

This work is partially supported by the National Science Council, Taiwan, R.O.C., under grant NSC 91-2214-E-155-009. The financial support is gratefully acknowledged.

Nomenclature

E_a = activation energy (J/mol)
g = process model [-]
h = constraint [-]
k_i = Kozeny−Carman parameter [-]
k_0 = rate constant (s^{-1})
L_x = length (m)
L_y = width (m)
L_z =height (m)
M = molecular weight (Kg/mol)
n = reaction order[-]
P = pressure (Pa)
P_0 = initial pressure (Pa)
R = gas constant (J/mol·k)
r = reaction rate (kg/m^3·s)
S = surface area per unit volume (m^{-1})
T = temperature (K)
T_0 = initial temperature (K)
t = time (s)
$\bar{t}$ = dimensionless time[-]
u = flow rate (m/s)
v_b = volumetric ratio of binder[-]
v_{b0} = initial volumetric ratio of binder[-]
v_{g0} = initial volumetric ratio of gas[-]
v_g = volumetric ratio of gas[-]
v_s = volumetric ratio of ceramic[-]
x = state variable[-]
α = conversion[-]
β = heating rate (K/min)
ρ_b = binder density (kg/m^3)
$\bar{\rho}$ = dimensionless gas density[-]

ρ = gas molar density (mole/m^3)
κ_i = permeability (m^2)
μ = viscosity (Pa·s)
γ = time constant (s)

Literature Cited

(1) Lewis, J. A. Binder Removal From Ceramics. *Annu. Rev. Mater. Sci.* **1997**, *27*, 147.

(2) Bonnet, E.; White, R. L. Effects of Water Vapor on Poly(vinyl butyral) Ceramic Binder Burnout. *J. Mater. Sci.* **2000**, *35*, 1787.

(3) Liau, L. C.-K.; Viswanath, D. S. Thermal Degradation of Poly(vinyl butyral)/Ceramic Composites: A Kinetic Approach. *Ind. Eng. Chem. Res.* **1998**, *37*, 49.

(4) Madras, G.; Smith J. M.; McCoy, B. J. Degradation of Poly(methyl methacrylate) in Solution. *Ind. Eng. Chem. Res.* **1996**, *35*, 1901.

(5) Liau, L. C.-K.; Liau, J.-Y. Kinetic Effects of Glass Ceramic and Silver on Poly(vinyl butyral) Thermal Degradation Using FT-IR. 1. *Ind. Eng. Chem. Res.* **2004**, *43*, 1938.

(6) Liau, L. C.-K.; Yang, T. C. K.; Viswanath, D. S. Mechanism of degradation of poly(vinyl butyral) using thermogravimetry/Fourier transform infrared spectrometry. *Polym. Eng. Sci.* **1996**, *36*, 2589.

(7) Liau, L. C.-K.; Liau, J.-Y.; Chen, Y.-T. Composition Effect of Glass Ceramic and Silver on Poly(vinyl butyral) Thermal Degradation Using Thermogravimetry Aanlysis. *J. Appl. Polym. Sci.* **2004**, *93*, 2142.

(8) Tsai, D. T. Pressure Buildup and Internal Stress During Binder Burnout: Numerical Analysis. *AIChE J.* **1991**, *37*, 547.

(9) Feng, K.; Lombardo, S. J. Modeling of the Pressure Distribution in Three-Dimensional Porous Green Bodies During Binder Removel. *J. Am. Ceram. Soc.* **2003**, *86*, 234.

(10) Feng, Z. C.; Lombardo, S. J. Stress Distribution in Porous Ceramic Bodies During Binder Burnout. *J. Appl. Mech.* **2002**, *69*, 49.

(11) Abel, O.; Helbig, A.; Marquardt, W.; Zwick, H.; Daszkowski, T. Productivity Optimization of an Industrial Semi-batch Polymerization Reactor Under Safety Constraints. *J. Process Control* **2000**, *10*, 351.

(12) Fournier, F.; Latifi, M. A.; Valentin, G. Methodology of Dynamic Optimization and Optimal Control of Batch Electrochemical Reactors. *Chem. Eng. Sci.* **1999**, *54*, 2707.

(13) Chen, B. H.; Bermingham, S.; Neumann, A. H.; Kramer, H. J. M.; Asprey, S. P. On the Design of Optimally Informative Experiments for Dynamic Crystallization Process Modeling. *Ind. Eng. Chem. Res.* **2004**, *43*, 4889.

(14) Liau, L. C.-K.; Hsieh, Y.-P. Kinetic analysis of poly(vinyl butyral)/glass ceramic degradation using nonlinear heating functions. *Polym. Degrad. Stab.,* in press.

Received for review September 6, 2004
Revised manuscript received February 13, 2005
Accepted April 25, 2005

IE049143A